



**HAL**  
open science

## Removal of Congo red by a synthesized layered double hydroxide ZN-AL-SO<sub>4</sub>

Messaadi Mahassene, M'Hamed Kaid, Ammam Abdelkader, Didier Villemin

► **To cite this version:**

Messaadi Mahassene, M'Hamed Kaid, Ammam Abdelkader, Didier Villemin. Removal of Congo red by a synthesized layered double hydroxide ZN-AL-SO<sub>4</sub>. International Journal of Ecosystems and Ecology Science, 2022, 10.31407/ijees12.229 . hal-03670177

**HAL Id: hal-03670177**

**<https://normandie-univ.hal.science/hal-03670177>**

Submitted on 17 May 2022

**HAL** is a multi-disciplinary open access archive for the deposit and dissemination of scientific research documents, whether they are published or not. The documents may come from teaching and research institutions in France or abroad, or from public or private research centers.

L'archive ouverte pluridisciplinaire **HAL**, est destinée au dépôt et à la diffusion de documents scientifiques de niveau recherche, publiés ou non, émanant des établissements d'enseignement et de recherche français ou étrangers, des laboratoires publics ou privés.

# REMOVAL OF CONGO RED BY A SYNTHESIZED LAYERED DOUBLE HYDROXIDE ZN-AL-SO<sub>4</sub>

Messaadi Mahassene<sup>1</sup>, Kaid M'hamed<sup>1</sup>, Ammam Abdelkader<sup>2\*</sup>, Didier Villemin<sup>3</sup>

<sup>1</sup>University of Saida Dr. Moulay Tahar, Laboratoire d'études physico-chimiques, Faculty of Sciences, Department of Chemistry, Box 138, Ennasr Saida. Algeria;

<sup>2\*</sup> University of Saida Dr. Moulay Tahar, Laboratory of biotoxicology, pharmacognosy and valorisation of plants, Faculty of Sciences, Department of Biology, Box 138, Ennasr Saida. Algeria ;

<sup>3</sup>Laboratoire de Chimie Moléculaire et Thioorganique. Ensicaen, UMR CNRS 6507, INC3M, FR 3038, 14050 Caen, France;

## ABSTRACT

The colored wastewaters from the textile industries may show toxic or carcinogenic effects on the organism, when discharged into the rivers and lakes, which are changing their biological life. Therefore, in this study, the removal of Congo red by Zn-Al-SO<sub>4</sub> layered double hydroxide has been achieved. Zn-Al-SO<sub>4</sub> material was prepared by a facile co-precipitation method at constant pH, resulting in a suitable material for the adsorption of Congo red dye. The structure and morphology of the Zn-Al-SO<sub>4</sub> adsorbent were investigated using XRD, FT-IR, and BET and MEB techniques. Layered double hydroxides (LDHs) have been widely investigated in a wide range of applications in health, in the pharmaceutical industry and in the material of biotechnology industries. In this work the synthesis of Zn/Al double layered hydroxides by chemical co-precipitation method (molar ration 3). The samples were characterized and confirmed by X-ray diffraction (XRD), BET analysis, and infrared spectroscopy. A series of experiments was then carried out to study the influence on the adsorption capacity of certain parameters such as the amount of the adsorbent, the pH, the contact time, the initial dye concentration, the ionic strength effect and temperature. All the results obtained show that the adsorption kinetics of the dye on our material is well described by the second order model. The adsorption isotherms of the adsorbent / adsorbate systems studied are satisfactorily described by the Langmuir mathematical model. The intra-particle scattering model confirms the physisorption phenomenon. Negative values of free energy prove that the phenomenon is physisorption. On the other hand, the thermodynamic study revealed that the adsorption is spontaneous and exothermic. The recovery of the material and reuse shows that the property of

being able to regenerate is remarkable.

**Key words:** LDH, Congo red, Adsorption, Regeneration.

## INTRODUCTION

Increasing environmental pollution caused by the rapid growth of technology is one of the serious concerns of global societies (Boulaiche et al., 2019). The growth of civilization and industrialization has led to the destruction of water resources (Järup., 2003; Niazi et al., 2009; Sajid et al., 2018). More than 10,000 dyes have been widely used in textile, rubber, paper, plastics, leather, cosmetic, pharmaceutical, and food industries, which generated huge volume of wastewater every year (Tahmasebi et al., 2015; Luo et al., 2015; Qu et al., 2017; Zhao et al., 2016). Annually the production of dyes is estimated at around 1.6 million tons which 10–15% of this amount is discharged to sewage. Exposure to these species causes skin irritation, respiratory problems, and cancer (Carro et al., 2015; Wang et al., 2016). In addition, the produced colored wastewater from the dye manufacturing and textile industries effects on biological life when is discharged into rivers and lakes without wastewater treatment. The long history of red coloring elements are figured out in two periods separated by a approximately recent year, 1858, marked by the invention of the first synthetic red dye. Previously, in the 19th century, foods were colored with natural red dyes, including cochineal red, beetroot red, madder, and metal salts as well. Yet, it had been merely following the invention of red dyes resulting from chemical synthesis that their use within the food industry spread from 1880. If the fields of application of red dyes remain very varied (the textile industry remains the main sector making use of these compounds), we note that since a few decades, the global food industry uses more and more significant amount of natural or artificial red dyes, in particular in confectionery, desserts, drinks, but also in cold cuts, fruits and vegetables and sugar. Otherwise, these compounds have a toxic character causing significant disturbances in the various natural mechanisms existing in the flora (self-purification power of watercourses, inhibition of the growth of aquatic plants, etc.) and in the fauna (destruction of a category of fish, microorganisms, etc.) (Alipour et al., 2021) and can persist a long time in this environment.

Besides to the toxicity and health risks of these pollutants, the wide kinds of red dyes usually have complex structure and non-biodegradable molecular due to their high molecular weight, so that is very hard to eliminate from environments (Gong et al., 2011). These are the reasons that the effective removal of these pollutants from water and their treatment before discharging into the water stream is a great

subject of research nowadays (Sajid et al., 2018). Different methods are used to remove organic pollutants, such as dyes from wastewater (Agarwal et al., 2017), like ozonation (Joshi et al., 2020), coagulation (Chen et al., 2010), electrocoagulation (Wang, K et al., 2016) photocatalytic removal (Ferrandon et al., 2001), membrane filter (Xu et al., 2015), and adsorption (Mnasri-Ghnimi et al., 2015; Naseem et al., 2019). Among various methods, and using a suitable adsorbent, adsorption is widely used as a reasonable technique due to its simplicity, ease of use, low cost, high efficiency and the availability of the materials (Lahreche et al., 2022).

The objective of this work is to prepare and characterize (ZnAl-SO<sub>4</sub>) by co precipitation method. This green adsorbent has been used to study the effects of different parameters on Congo red adsorption, such as pH of the aqueous solution, quantity of hybrid material, initial concentration of heavy metal ion, adsorption equilibrium time, stirring speed, salts effects and temperature.

## **MATERIAL AND METHOD**

### ***Experimental Materials***

The reagents used in this study were Zn Al-SO<sub>4</sub> synthesized in the laboratory (Kadari et al., 2017; Mahassene et al., 2016), the raw materials ZnSO<sub>4</sub> (Riedel De Haen), Al<sub>2</sub>(SO<sub>4</sub>)<sub>3</sub> (Riedel De Haen), nitric acid (64% Riedel De Haen), Congo red (98%, Sigma Aldrich), NaOH (99%, Riedel De Haen), Na<sub>2</sub>SO<sub>4</sub>, KNO<sub>3</sub> (99%, Riedel De Haen), UV/Vis spectra were obtained using a UV/Visible double beam type" OPTEZEN 3220" spectrometer to analyze the concentration of congo red in aqueous solution, a digital pH meter Consort C863 type.

### ***Methods***

#### ***Synthesis of the ZnAlSO<sub>4</sub>***

Zn-Al-SO<sub>4</sub> was prepared using a co-precipitation method similar to that described by Miyata (Miyata., 1975) with a Zn/Al ratio of 3 a. In a reactor, 150 mL of an aqueous solution of metallic sulphates (0.75 M in ZnSO<sub>4</sub> and 0.25 M in Al<sub>2</sub>(SO<sub>4</sub>)<sub>3</sub>) was added drop wise, at 25°C and under magnetic stirring. 1.5 M NaOH was added to maintain the pH of the reaction mixture constant at 10.5 ± 0.1. When the reaction was achieved, the resultant gel was made under reflux at 60-70°C during 15 hours to permit crystal growth. After ripening, at room temperature for 24 h in mother liquors, the mixture was filtered, washed several times then dried, a white precipitate was obtained.

#### ***Adsorption experiment***

The LDH of type ZnAl-SO<sub>4</sub> with a molar ratio of 3 has been prepared by the method of co-precipitation described by Miyata. In this work, we have chosen the method of spectrophotometry molecular absorption as colorful indicator for the determination of Congo red at  $\lambda_{\max} = 500$  nm (Guiza et al., 2022)

Several mixtures of solid phase (ZnAl-SO<sub>4</sub>) and aqueous phase of the dye are subjected to magnetic stirring. After separating the two phases by centrifugation, the amount of Congo red remaining in the aqueous phase has been determined by spectrophotometry visible UV/V (double beam type" OPTEZEN 3220" spectrometer), The amounts of Congo red adsorbed are calculated from the following equation (1):

$$q_e = \frac{(C_0 - C_e)V}{m} \quad (1)$$

Where C<sub>0</sub> and C<sub>e</sub> are the initial and equilibrium concentrations of Congo red (mg L<sup>-1</sup>) respectively; m the amount of adsorbent (g) and V the volume of solution (L). The efficiency percentage (Y) of dye removal was calculated as follows (equation (2):

$$Y\% = \frac{(C_0 - C_e)}{C_0} \times 100 \quad (2)$$

### ***Characterization techniques***

#### ***XRD Analyses***

Powder X-ray diffraction (XRD) data were collected on a PANAnalytical X'Pert Pro diffractometer in reflection mode at 40 kV and 40 mA using Cu K $\alpha$  radiation (1.5405980 Å). Scans were recorded from 5° ≤ 2θ ≤ 100° with varying scan speeds and slit sizes. Samples were mounted on stainless steel sample holders.

#### ***FTIR Analyses***

Fourier transform infrared (FTIR) spectra were recorded using a Perkin Elmer 16 PC-FTIR equipped with a thermostat to maintain the temperature of the sample at 25.0 ± 01 °C on KBr pellets in the range of 4000-400 cm<sup>-1</sup>.

#### ***BET analyses***

Specific surface areas and pore size were analyzed using the Brunauer–Emmett–Teller (BET) method. The samples were measured from the N<sub>2</sub> adsorption and desorption isotherms at 77 K collected from a Quantachrome Autosorb-6 surface area and pore size analyzer.

### ***UV/V analyses***

A UV/Visible double beam type "OPTEZEN 3220" spectrometer was used for UV-vis spectral measurements.

The accuracy and the precision of the method on the instrument were determined by measuring the absorbance at 500 nm against the prepared standards in the concentration range of ( $10^{-3}$  to  $10^{-6}$  mol/l) (Chen et al., 2010). A standard curve for UV-vis measurement demonstrated high degree of accuracy with a coefficient of regression,  $R^2=99.7$  %, was used in the calculation of unknown UV-vis concentrations from absorbance readings.

## **RESULTS AND DISCUSSION**

### ***X-ray diffraction***

The powder XRD pattern of Zn-Al-SO<sub>4</sub> is presented in figure (Figure 1). The diffraction peaks corresponding to the LDH phase are observed at the  $2\theta$  position 12.4, 20, 27.5, 37.2, 42. and 47.1 having the respective  $d$ -values 10.94, 5.47, 3.66, 2.66 and 2.18 and the respective miller indices are 003, 006, 015, 018, 110 and 113 characteristic of an LDH phase with a basal spacing of 7.98 Å and an inter metallic distance of 1.52 Å. The XRD patterns corresponding to the rhombohedral symmetry (space group, R-3m) are indexed in an hexagonal lattice. The (a) and (c) lattice parameters are estimated using (110) and (003) reflections, respectively.

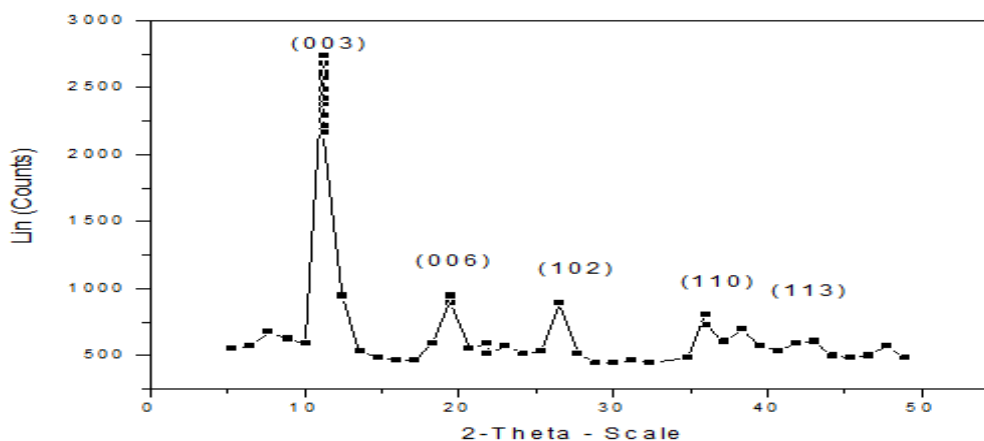


Figure 1. DRX pattern of ZnAl-SO<sub>4</sub>

### ***Fourier transformed infrared spectroscopy analysis (FTIR)***

The spectra FTIR of ZnAl-SO<sub>4</sub> is shown in Figure 2. The presence a very intense band peak around 3458  $\text{cm}^{-1}$  corresponds to the vibration of the hydroxide

groups of the molecules water. The band recorded at  $1620\text{ cm}^{-1}$  can be assigned to intercalated water molecules deformation. Lattice vibrations appear in the  $430\text{-}559\text{ cm}^{-1}$  range. The weak band at  $2100$  indicates the binding vibration of  $\text{SO}_4^{2-}$ . The band at  $1352\text{ cm}^{-1}$  indicates the presence of small amounts of carbonate in the galleries (Delgado et al., 2008).

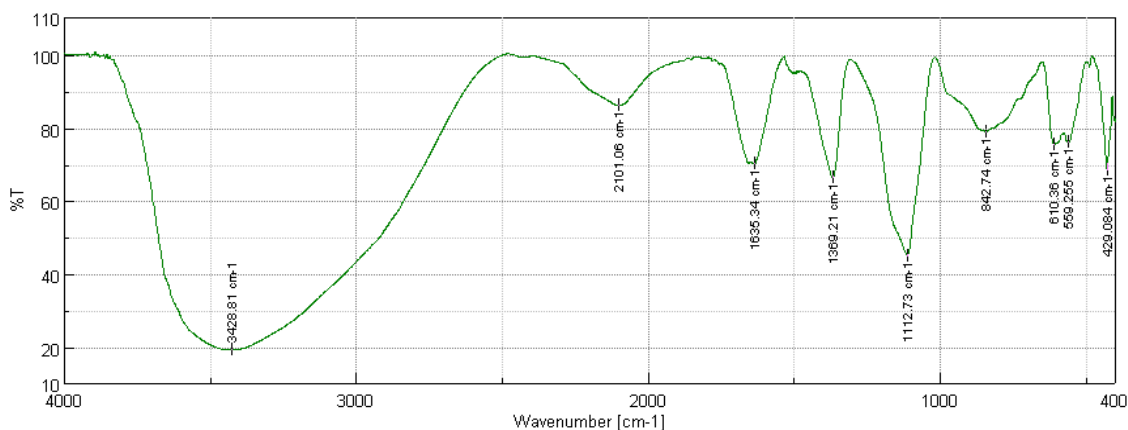


Figure 2. FTIR spectrum of Zn-Al-SO<sub>4</sub>

### Specific area

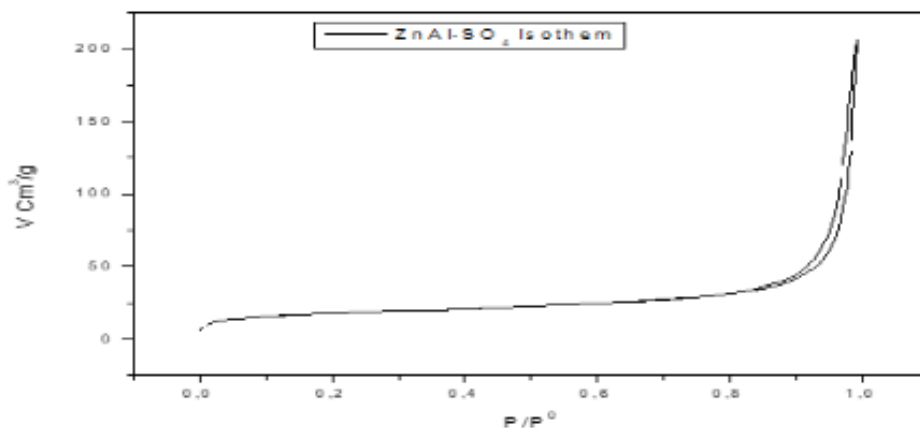


Figure 3. Adsorption isotherm for ZnAl-SO<sub>4</sub>

Table 1. Pore properties and specification surface area of ZnAl-SO<sub>4</sub>

	BET surface area ( $\text{m}^2\text{g}^{-1}$ )	Pore volume ( $\text{cm}^3\text{g}^{-1}$ )	Average pore size (nm)
Zn/Al-LDH	62.5	0.29	18.6

## ***Morphology***

SEM images of ZnAl-SO<sub>4</sub>-LDH are presented in Figure 4. The images clearly show that the sample existing lamellar particles with hexagon layer structure, which is the typical structure of the hydrotalcite-like material.

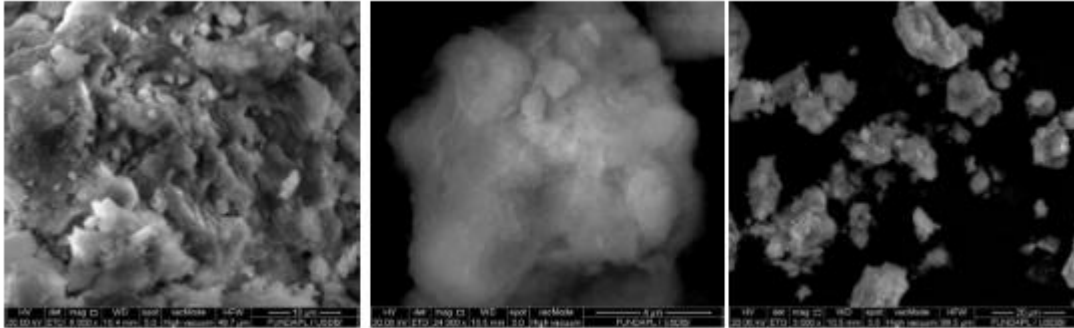


Figure 4. SEM image of ZnAl-SO<sub>4</sub>

## ***Effect of various parameters on Congo red dye removal efficiency***

Different parameters have been investigated to study the retention yield of Congo red dye

### ***Effect of stirring speed***

We observe that the adsorption rate depends on the stirring speed. On the other hand, it is fast for  $t < 10$  min, then it remains constant (Figure 5). The agitation speed affects the resistance to the transfer of material outside the clay particle, this with accordance with literature (Guiza et al., 2019).

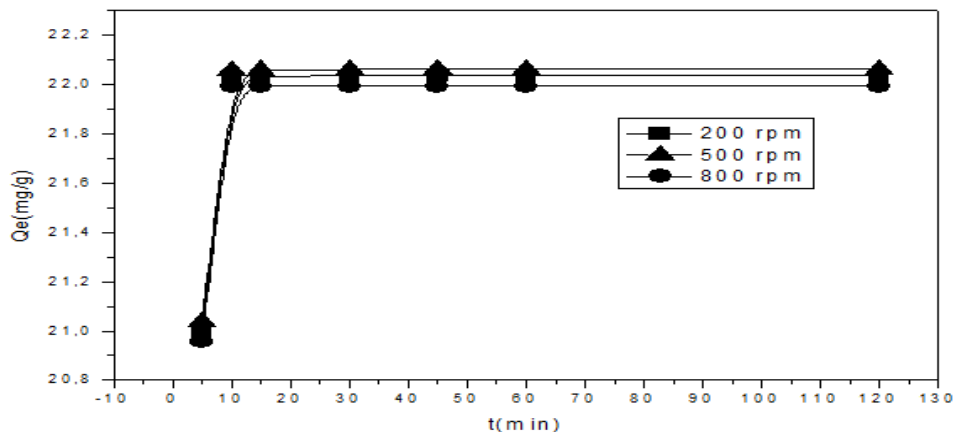


Figure 5. Effect of stirring speed on the retention of Congo red

$M = 0,025\text{g}$  et  $C=55,74\text{ mg/L}$  . $T=25^{\circ}\text{C}$

### ***Effect of material amount on the efficiency of Congo red removal***

Three volumes of the dye solution with 55,74 mg/L has been prepared and added to



four different amounts of ZnAl- SO<sub>4</sub> LDH: 0.025, 0,035, 0.045 and 0.055 g. The best yield has been obtained with a mass 0.025 g reaching 99,9 % with average stirring speed of 500 rpm as shown in the graphical representation on figure 6. This is explained by the attainability of the sites of the adsorbent. The mass transfer of the dye in the external film can be controlled by the LDH amount; the increase in the LDH dose contributes to the increase of the transfer coefficient in the liquid film.

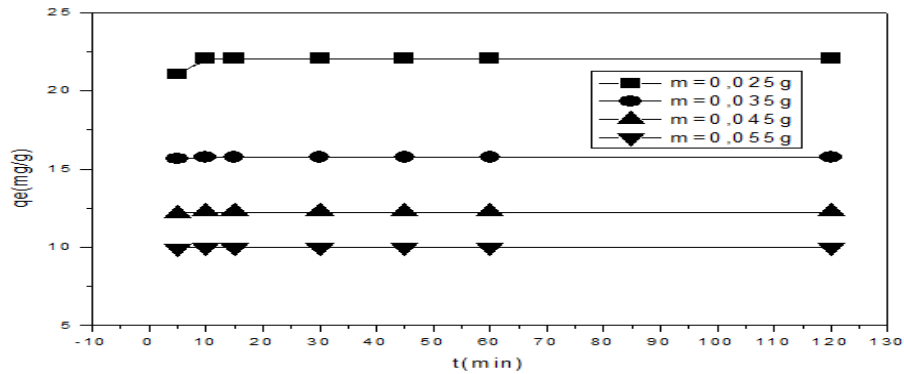


Figure 6. Adsorbent amount effect on the Congo red retention

$$T=25C^{\circ}, [Dye] = 55,74 \text{ mg/L}$$

### *Effect of dye concentration on the removal efficiency*

Various concentrations of congo red dye was used: 5.57, 34.83 and 55.74 mg/L with an amount of (ZnAl-SO<sub>4</sub>) adsorbent 0.025 g. and under 500 rpm. The results are presented in Figure 7. It has been shown that the best retention yield is obtained with a concentration 55, 74 mg/l. The results are gathered in figure 7.

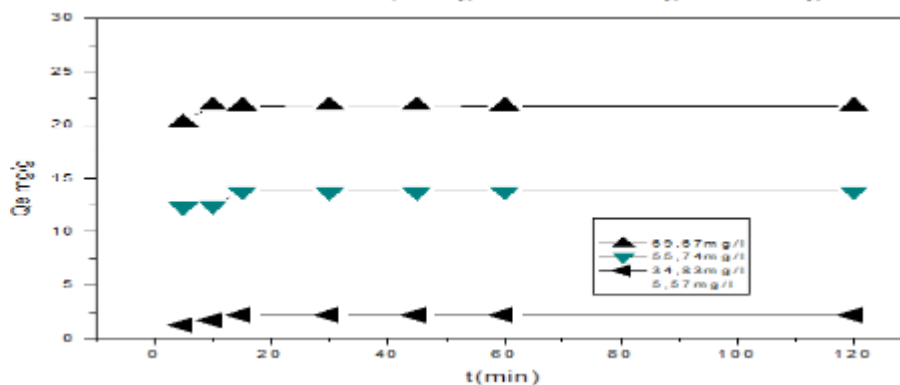


Figure 7. Concentration effect on the retention of Congo red. T = 25C<sup>°</sup>, m = 0,025 g

### *Effect of pH on the efficiency of Congo red removal*

The removal of Congo red has been investigated in the pH range from 3.5 to 12 by adding nitric acid HNO<sub>3</sub> in different solutions with an adsorbent dose of 0.025 g. According to the results shown in Figure 8, we noted that the removal of dye by

the ZnAl-SO<sub>4</sub> is much more important at pH=8 with best adsorption capacity of 23 mg/g. That is to say the more acidic (pH = 3.5) is the solution, the less dye are extracted. This is probably due either to competition between the ionic organic pollutant dye in solution and the ions released by the nitric acid or to the non- stability of the LDH in acidic solution.

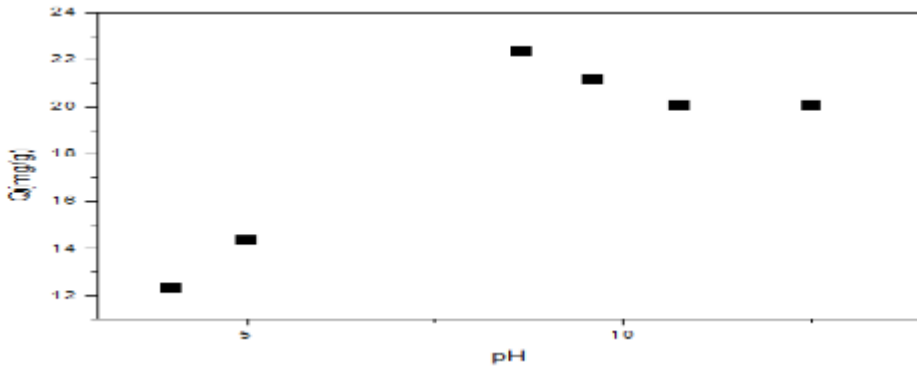


Figure 8. Effect of initial solution pH on the dye retention. T=25C°, m=0,025 [dye] = 55,74 mg/L

### *Effect of temperature on the efficiency of Congo red removal*

The effect of temperature on the extraction yield has been studied in the temperature range from 40 to 60°C. Thermodynamic parameter, free energy ( $\Delta G^\circ$ ), enthalpy ( $\Delta H^\circ$ ) and entropy ( $\Delta S^\circ$ ) have been determined; by the application, at the extraction equilibrium, of the following thermodynamic relations (Mahassene et al.,2016):

$$\Delta G^\circ = \Delta H^\circ - T\Delta S^\circ \quad (3)$$

$$\ln \Delta G^\circ = -RT \ln K_d \quad (4)$$

From these two equations, the following expression was obtained:

$$\ln k_d = \frac{\Delta S^\circ}{R} - \frac{\Delta H^\circ}{RT} \quad (5)$$

The calculation of certain thermodynamic parameters is essential in determining the nature of the retention process. The equilibrium constant K<sub>d</sub>, can be calculated from the following relation:

$$K_d = \frac{q_e \left(\frac{m}{V}\right)}{[C_0 - q_e \frac{m}{V}]} \quad (6)$$

The capacity of adsorption (q) of the studied heavy metals by the LDH is determined by the following relation

$$q(\text{mg/g}) = \frac{(C_0 - C_e) \cdot V \cdot M}{m} \quad (7)$$

$q_e$ : the capacity of the adsorption at equilibrium  
 $C_0$ : initial concentration of Congo red in mg/L  
 $C_e$ : the concentration of the Congo red at equilibrium in mol/L  
 $V$ : the volume of the solution of the treated Congo red (10 mL)  
 $M$ : the molar mass of Congo red dye  
 $m$ : the mass of ZnAl-SO<sub>4</sub> (0.025 g)  
 $R$ : the perfect gas constant ( $R = 8.314 \text{ J mol}^{-1} \text{ K}^{-1}$ )  
 $K_d$ : the distribution coefficient between the aqueous and solid phases

The thermodynamics parameters are listed in Table 2, where  $\Delta G^0$  values were obtained by plotting  $\ln K$  against  $1/T$  for the Langmuir data.

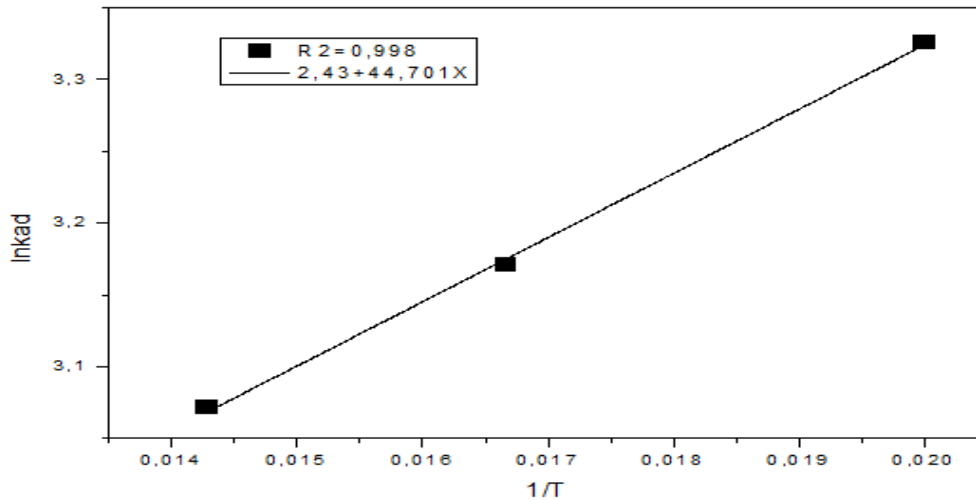


Figure 9.  $\ln K_{ads}$  function of  $1/T$  for the Congo red retention

The results of the thermodynamic study show that in (Table 2):

The negative  $\Delta H^\circ$  value indicates the exothermic nature of adsorption of the Congo red and was less than 10 kcal/mol indicating physical adsorption. The  $\Delta G^\circ$  values obtained were negative meaning that the adsorption was spontaneous and positive value of  $\Delta S^\circ$  suggested a slight increase in the randomness at the solid/solution interface during adsorption of dye on to the adsorbent.

Table 2. Adsorption Thermodynamic parameters at 303K

Thermodynamic Parameters	$\Delta G^\circ$ (kcal. mol <sup>-1</sup> )	$\Delta H^\circ$ , (kcal.mol <sup>-1</sup> )	$\Delta S^\circ$ (cal.m <sup>-1</sup> .kcal <sup>-1</sup> )
Values	-1.55	-0.088	4.83

### **Adsorption isotherm**

The study of the adsorption isotherm is fundamental and plays an important

role in determining the maximal capacity of adsorption. In order to adapt for the considered system, an adequate model that can reproduce the experimental results obtained, Langmuir, Freundlich and Dubinin-Radushkevich models have been considered.

In Figure 10, the quantities adsorbed according to the concentrations of the aqueous solution in equilibrium shows that the isotherm is of L-type which is obtained when the adsorption of the solvent is low and when the molecules are not oriented vertically but rather flat. In this case, the adsorption of the solute on the solid takes place in a monolayer.

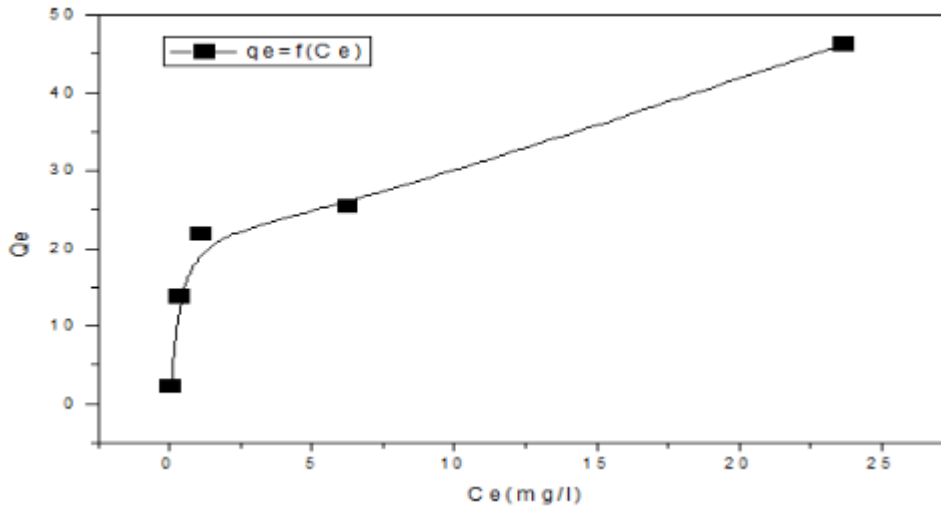


Figure 10. Graphical representation of the isotherm of the Congo red aqueous solution

### ***Langmuir isotherm model***

Mathematically, Linearization of Langmuir isotherm model is defined as:

$$\frac{1}{q_e} = \frac{1}{q_m \cdot K_L \cdot C_e} + \frac{1}{q_m} \quad (8)$$

Where  $q_m$  is the monolayer capacity of the adsorbent, and  $K_L$  is the Langmuir adsorption constant.  $q_m$  and  $K_L$  can be determined from the slope and intercept, respectively from the plot of  $1/q_e$  versus  $1/C_e$  (figure 11).

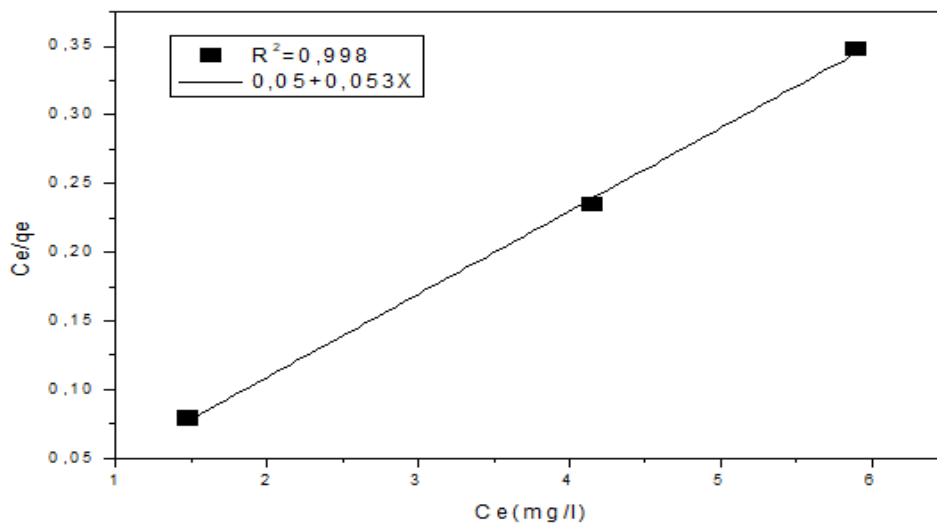


Figure 11. Langmuir linearization

### *Freundlich isotherm model*

This model describes systems where the adsorption is done on heterogeneous surfaces with interactions between the adsorbed molecules; the linear form is given by:

$$\log q_e = \log K_f + 1/n \log C_e \quad (9)$$

The constant ( $K_f$ ), due to the bond energy, and the heterogeneity factor ( $1/n$ ) which measures the deviation from the linear part are determined from the plot  $\log q_e$  versus  $\log C_e$ . The experimental results obtained at ambient temperature are presented in Figure 12. The Freundlich equation (8) is applied for the adsorption of the Congo red dye on our prepared LDH.

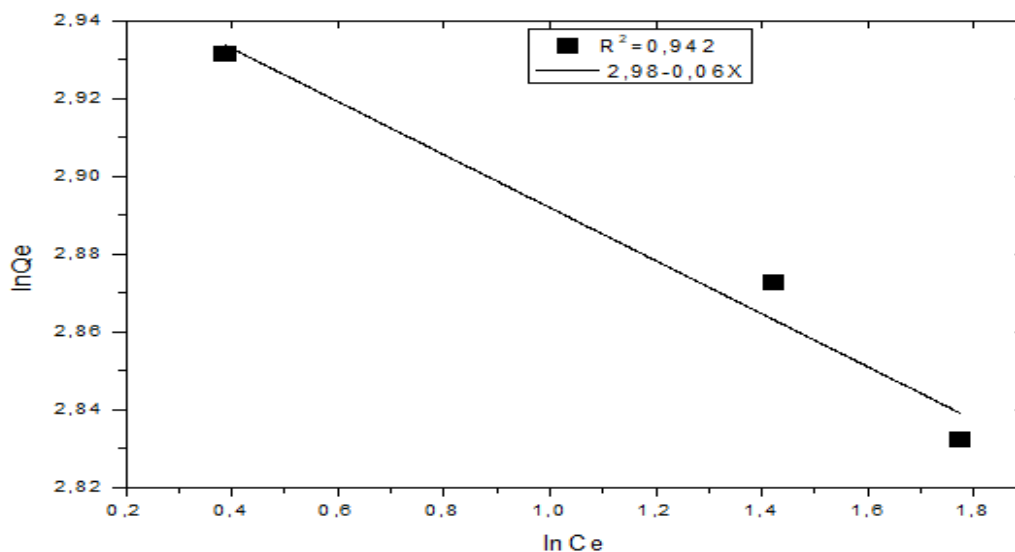


Figure 12. Freundlich linearization

Table 3. Langmuir and Freundlich constants for the elimination of Congo red on ZnAl-SO4

Langmuir model		Freundlich model	
Qm (mg/g)	KL (l/mg)	1/n	KF
22.22	0.52	-0.023	21.75

### ***Dubinin – Radushkevich Isotherm***

Plotting  $\ln q_e = f(\epsilon^2)$  gives us the line of the slope  $\beta$ , and  $q_s$  is the y-intercept. The results obtained are gathered in Table 4 and Figure 13 shows a linear adjustment.

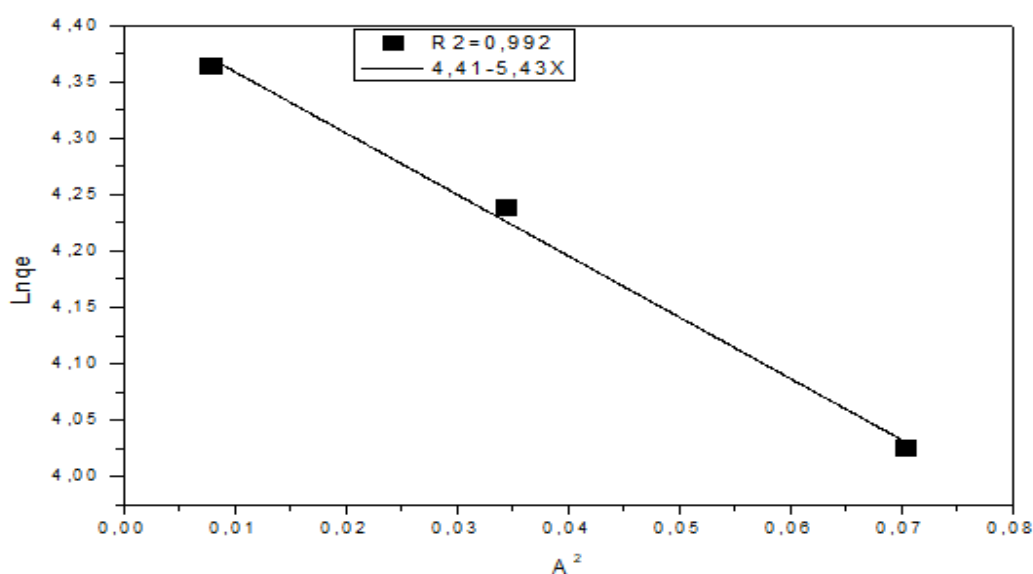


Figure 13. Dubinin–Radushkevich model for dye retention

Table 4. Dubinin–Radushkevich parameters for the elimination of Congo red on ZnAl-SO4

Dubinin Radushkevich model			
$q_s$ (mg/g)	$\beta$ ( $\text{mol}^2 \cdot \text{kJ}^{-2}$ )	E (kJ/mol)	$R^2$
82,27	5,43	0,130	0,992

These values indicate the predominance of physical adsorption ( $E < 8$  kJ/mol)

### ***Kinetic study***

The kinetic adsorption of Congo red dye by ZnAl-SO4 is studied at different contact times in the batch system and has been tested with pseudo first order pseudo second order and Intra particles diffusion model.

### ***Pseudo-first-order model***

The fitting results based on the pseudo-first order kinetic model are shown in Figure 14. The values for the kinetic models are shown in Table 5

$$\ln(q_e - q_t) = \ln q_e - k_1 t \quad (10)$$

Where  $q_e$  and  $q_t$  refer to the amount of mercury adsorbed per unit weight of Zn-Al-SO<sub>4</sub> respectively at equilibrium and at any time:

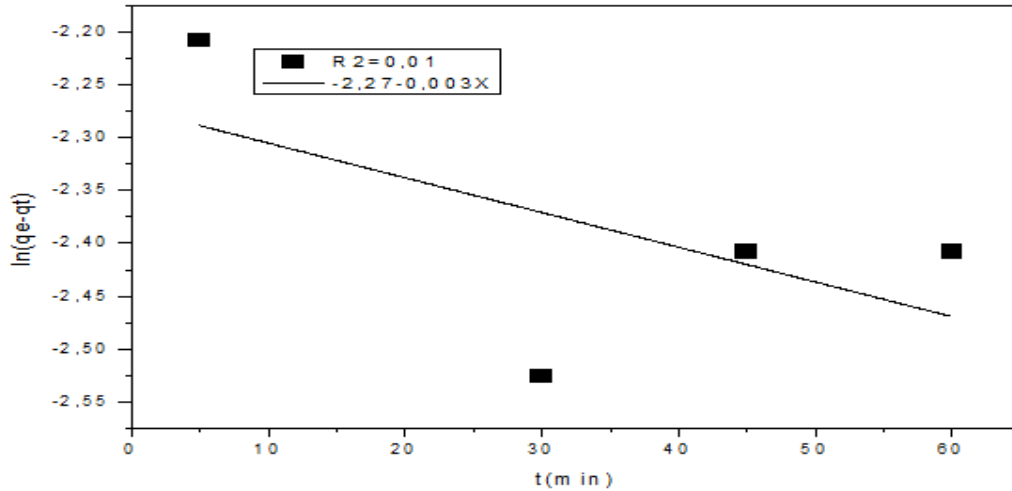


Figure 14. Kinetics of pseudo first-order for congo red retention

### ***Pseudo-second-order***

Using the pseudo-second-order equation also, the adsorption process may be described. The differential equation is the following:

$$\frac{t}{q_t} = \frac{1}{K_2 q_{eq}^2} + \frac{1}{q_{eq}^2} t \quad (11)$$

The results obtained (Figure 15) show that the pseudo-second-order model is more suitable to describe the kinetics of the retention of Congo red toxic dye by ZnAl-SO<sub>4</sub>.

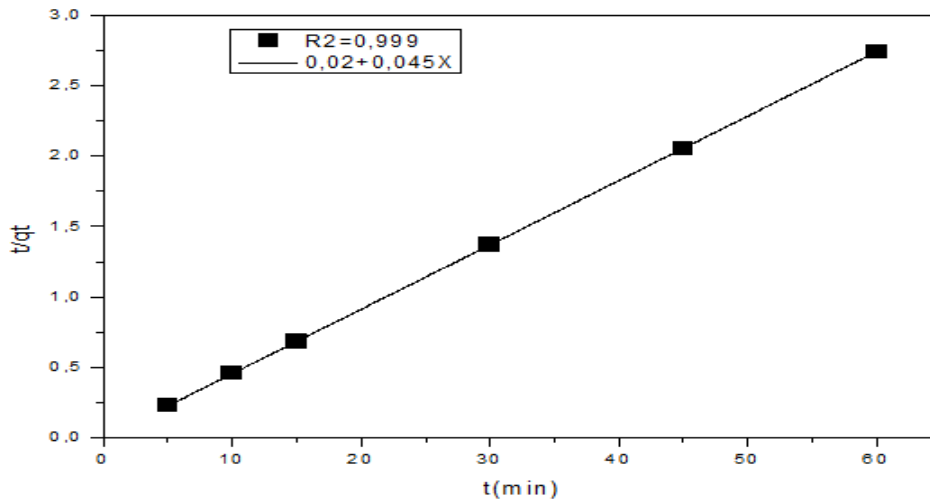


Figure 15. Kinetics of pseudo second order for Congo red retention

### *Intra particles diffusion model*

Solute transfer is generally characterized by either the external mass transfer step or intra particle diffusion or both. To study the existence of intraparticle diffusion during adsorption, the most widely used equation (12) is that given by (Abdel-Ghani et al ., 2016).

$$q_e = K_1 C^{0.5} + C \quad (12)$$

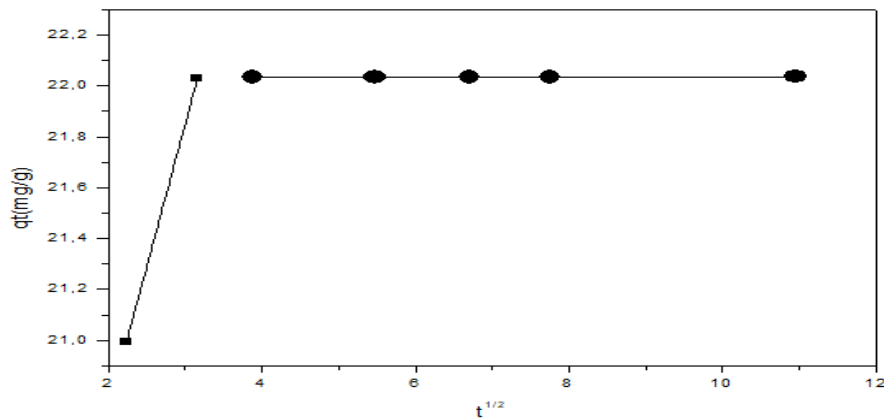


Figure 16. Diffusion model of Congo red dye particles

From figure 16, we distinguish a double linearity reflecting the existence of two stages: firstly, the high adsorption rate, resulting from the diffusion of the outer film and through the boundary layer of the outer surface of the adsorbent. Second, the adsorption process is controlled by intra-particle diffusion, which is characterized by slowing the rate of adsorption, and it is known as the rate-limiting step. These two phases are involved simultaneously during adsorption.



	Qe exp (mg/g)	K <sub>1</sub> (l/min),K <sub>2</sub> (g/min .mg)		Qe (mg/g)	R <sup>2</sup>
Pseudo 1 <sup>st</sup> order	22,08	0,003		0,10	0,01
Pseudo 2 <sup>nd</sup> order	22,08	9,87		22,22	0,999
diffusion model	Qe exp(mg/g)	Kint(mg/g /min <sup>1/2</sup> )		Ci(mg/g)	R <sup>2</sup>
Step 1	22,03	3,55×10 <sup>-4</sup>		22,03	0,97
Step 2	22,03	1,12		18,50	-

### **Material Regeneration**

The economic and environmental aspect of the use of adsorbent materials makes it important to reuse anionic clays, given their low cost and their ability to regenerate. After an adsorption with a yield R of almost 100%, desorption has been carried out using a solution of NaOH of known concentration  $C = 5 \times 10^{-3}$  M which is chosen after many trials using different NaOH concentrations.

The material used has been used for seven cycles showing best performance at each cycle.

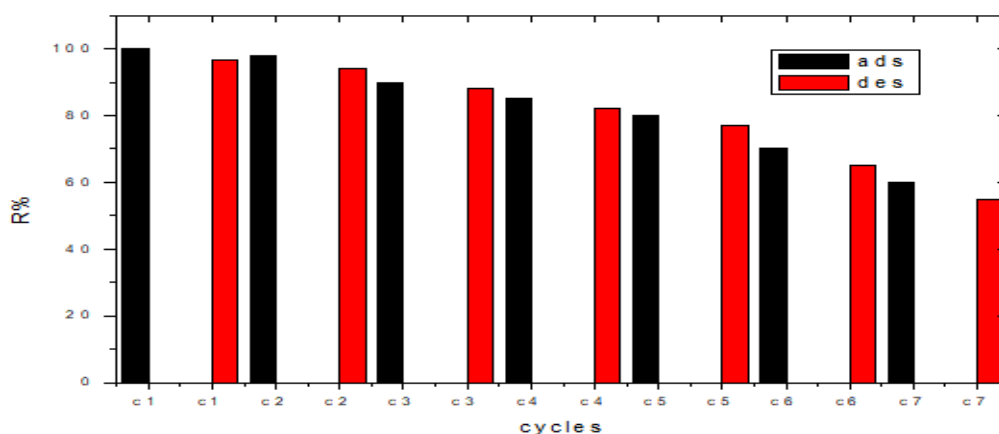


Figure 17. Recycling and reuse of ZnAl-SO<sub>4</sub> towards adsorption of Congo red

### **CONCLUSION**

Our prepared material (ZnAl-SO<sub>4</sub>) was found very effective adsorbent for the removal of Congo red dye from aqueous solutions. The synthetic method used to synthesize this adsorbent by chemical co-precipitation method is highly efficient and very low cost. This compound adsorbent showed that elimination can reach 100% under the optimal conditions and can be used at least for seven cycles. This can allow us to provide this adsorbent (Zn-AlSO<sub>4</sub>) for the waste water treatments.

**Acknowledgements.** This work was supported by Dr Moulay Tahar University, Saida, Algeria and “PunchOrga” Network (Pole Universitaire Normand de Chimie Organique), the “Ministère de la Recherche et des Nouvelles Technologies,” CNRS (Centre National de la Recherche Scientifique).

## REFERENCES

1. Abdel-Ghani, N., Rawash, E., & El-Chaghaby, G. (2016). Equilibrium and kinetic study for the adsorption of p-nitrophenol from wastewater using olive cake based activated carbon. *Global Journal of Environmental Science and Management*, 2(1), 11-18;
2. Agarwal, M., & Singh, K. (2017). Heavy metal removal from wastewater using various adsorbents: a review. *Journal of Water Reuse and Desalination*, 7(4), 387-419;
3. Alipour, M., Vosoughi, M., Mokhtari, S. A., Sadeghi, H., Rashtbari, Y., Shirmardi, M., & Azad, R. (2021). Optimising the basic violet 16 adsorption from aqueous solutions by magnetic graphene oxide using the response surface model based on the Box–Behnken design. *International Journal of Environmental Analytical Chemistry*, 101(6), 758-777;
4. Boulaiche, W., Hamdi, B., & Trari, M. (2019). Removal of heavy metals by chitin: equilibrium, kinetic and thermodynamic studies. *Applied Water Science*, 9(2), 1-10;
5. Carro, L., Barriada, J. L., Herrero, R., & de Vicente, M. E. S. (2015). Interaction of heavy metals with Ca-pretreated Sargassum muticum algal biomass: Characterization as a cation exchange process. *Chemical Engineering Journal*, 264, 181-187;
6. Chen, Y., Pan, B., Li, H., Zhang, W., Lv, L., & Wu, J. (2010). Selective removal of Cu (II) ions by using cation-exchange resin-supported polyethyleneimine (PEI) nanoclusters. *Environmental science & technology*, 44(9), 3508-3513;
7. Delgado, R. R., De Pauli, C. P., Carrasco, C. B., & Avena, M. J. (2008). Influence of MII/MIII ratio in surface-charging behavior of Zn–Al layered double hydroxides. *Applied Clay Science*, 40(1-4), 27-37;
8. Ferrandon, O., & Bouabane, H. (2001). Influence d'alcools aliphatiques sur l'adsorption d'acides aminés sur charbon actif. *Comptes Rendus de l'Académie des Sciences-Series IIC-Chemistry*, 4(12), 879-883;
9. Gong, J., Liu, T., Wang, X., Hu, X., & Zhang, L. (2011). Efficient removal of heavy metal ions from aqueous systems with the assembly of anisotropic layered double hydroxide nanocrystals@ carbon nanosphere. *Environmental science & technology*, 45(14), 6181-6187;
10. Guiza, S., Hajji, H., & Bagane, M. (2019). External mass transport process during the adsorption of fluoride from aqueous solution by activated clay. *Comptes Rendus Chimie*, 22(2-3), 161-168;
11. Guiza, S. & Bagane, M. (2022) Kinetics study of Congo red dye adsorption from aqueous solutions onto bentonite; *Journal of Water Science*. 10:07;
12. Järup, L. (2003). Hazards of heavy metal contamination. *British medical bulletin*, 68(1), 167-182;
13. Joshi, N. C., Malik, N., & Singh, A. (2020). Synthesis and characterizations of polythiophene–Al<sub>2</sub>O<sub>3</sub> based nanosorbent and its applications in the removal of Pb<sup>2+</sup>, Cd<sup>2+</sup> and Zn<sup>2+</sup> ions. *Journal of Inorganic and Organometallic Polymers and Materials*, 30(4), 1438-1447;
14. Kadari, M., Kaid, M. h., Ben Ali, M., & Villemin, D. (2016). The intercalation of Zn/Al-HDL by the diamino-dodecylphosphonic acid: synthesis and properties of adsorption of basic fuchsin. *Journal of the Chinese Advanced Materials Society*, 4(2), 148-157;
15. Lahreche, S., Moulefera, I., El Kebir, A., Sabantina, L., Kaid, M., & Benyoucef, A. (2022). Application of Activated Carbon Adsorbents Prepared from Prickly Pear Fruit Seeds and a Conductive Polymer Matrix to Remove Congo Red from Aqueous Solutions. *Fibers*, 10(1), 7;
16. Luo, J., Luo, X., Crittenden, J., Qu, J., Bai, Y., Peng, Y., & Li, J. (2015). Removal of antimonite (Sb (III)) and antimonate (Sb (V)) from aqueous solution using carbon nanofibers that are decorated with zirconium oxide (ZrO<sub>2</sub>). *Environmental science & technology*, 49(18), 11115-11124;
17. Mahassene, M., M'hamed, K., Mohamed, K., Ali, M. B., & Villemin, D. (2016). The intercalation of Zn/Al HDL by diaminododecylphosphonic acid: synthesis and properties of adsorption of cadmium. *Adv. Mater. Manu Charac.*, 6(1), 21-28;
18. Miyata, S. (1975). The Syntheses of Hydrotalcite-Like Compounds and Their Structures and Physico-Chemical Properties—I: The Systems Mg<sup>2+</sup>-Al<sup>3+</sup>-NO<sub>3</sub><sup>-</sup>, Mg<sup>2+</sup>-Al<sup>3+</sup>-Cl<sup>-</sup>, Mg<sup>2+</sup>-Al<sup>3+</sup>-ClO<sub>4</sub><sup>-</sup>, Ni<sup>2+</sup>-Al<sup>3+</sup>-Cl<sup>-</sup> and Zn<sup>2+</sup>-Al<sup>3+</sup>-Cl<sup>-</sup>. *Clays and Clay Minerals*, 23(5), 369-375;
19. Mnasri-Ghnimi, S., & Frini-Srasra, N. (2019). Removal of heavy metals from aqueous solutions by adsorption using single and mixed pillared clays. *Applied Clay Science*, 179, 105151;
20. Naseem, K., Begum, R., Wu, W., Usman, M., Irfan, A., Al-Sehemi, A. G., & Farooqi, Z. H. (2019). Adsorptive removal of heavy metal ions using polystyrene-poly (N-isopropylmethacrylamide-acrylic acid) core/shell gel particles: adsorption isotherms and kinetic study. *Journal of Molecular Liquids*, 277, 522-531;
21. Niazi, A., Momeni-Isfahani, T., & Ahmari, Z. (2009). Spectrophotometric determination of mercury in water samples after cloud point extraction using nonionic surfactant Triton X-114. *Journal of Hazardous Materials*, 165(1-3), 1200-1203;
22. Qu, Z., Fang, L., Chen, D., Xu, H., & Yan, N. (2017). Effective and regenerable Ag/graphene adsorbent for Hg (II) removal from aqueous solution. *Fuel*, 203, 128-134;
23. Sajid, M., Nazal, M. K., Baig, N., & Osman, A. M. (2018). Removal of heavy metals and organic pollutants from water using dendritic polymers based adsorbents: a critical review. *Separation and Purification Technology*, 191, 400-423;

24. Tahmasebi, E., Masoomi, M. Y., Yamini, Y., & Morsali, A. (2015). Application of mechanosynthesized azine-decorated zinc (II) metal–organic frameworks for highly efficient removal and extraction of some heavy-metal ions from aqueous samples: a comparative study. *Inorganic chemistry*, *54*(2), 425-433;
25. Wang, K., Zhao, J., Li, H., Zhang, X., & Shi, H. (2016). Removal of cadmium ( II) from aqueous solution by granular activated carbon supported magnesium hydroxide. *Journal of the Taiwan Institute of Chemical Engineers*, *61*, 287-291;
26. Wang, Q., Shi, X., Xu, J., Crittenden, J. C., Liu, E., Zhang, Y., & Cong, Y. (2016). Highly enhanced photocatalytic reduction of Cr (VI) on AgI/TiO<sub>2</sub> under visible light irradiation: influence of calcination temperature. *Journal of Hazardous Materials*, *307*, 213-220;
27. Xu, Z., Gao, G., Pan, B., Zhang, W., & Lv, L. (2015). A new combined process for efficient removal of Cu (II) organic complexes from wastewater: Fe (III) displacement/UV degradation/alkaline precipitation. *Water research*, *87*, 378-384;
28. Zhao, D., Yu, Y., & Chen, J. P. (2016). Treatment of lead contaminated water by a PVDF membrane that is modified by zirconium, phosphate and PVA. *Water research*, *101*, 564-573 ;